Granular Memristors with Tunable Stochasticity

Uddipan Ghosh[a], Ankur Bhaumik[a], Navyashree Vasudeva[a], Anshu Pandey[a]

[a]Solid State And Structural Chemistry Unit, Indian Institute of Science

Supplementary Information

Section 1 (Synthesis and Device Fabrication):

Materials: Hexadecyltrimethylammoniumbromide (CTAB) (≥98%) from Sigma Aldrich, Silver nitrate ($AgNO_3$) (ACS reagent, ≥ 99.0%) from Sigma-Aldrich, sodium borohydride ($NaBH_4$) powder from SigmaAldrich (≥98.0%), hydrogentetrachloroaurate(III)trihydrate ($HAuCl_4.3H_2O$) from Sigma-Aldrich (ACS, 99.99% pure, metal basis) and L-Ascorbic acid (99%, Sigma Aldrich) were used as received without any further purification. All the aqueous solutions have been prepared in 18.2 M-Ohm milli-Q water to avoid contamination.

Synthesis of Au Nanospheres:

Gold nanospheres with sizes ranging from 20-30 nm were synthesized using a seed-mediated process. Initially, a solution was prepared by mixing 5 mL of 0.5 mM $HAuCl_4$ with 5 mL of 0.1 M CTAB, which was vigorously stirred. Subsequently, 0.6 mL of 0.01 M $NaBH_4$ was added to this mixture, resulting in a brownish solution indicative of gold nanocrystal formation. These nanocrystals served as seeds for further growth.

To synthesize 20-30 nm gold nanospheres, a 500 mL growth solution was prepared containing 5 mM $HAuCl_4$, 0.1 M CTAB in 500 mL water. To this growth solution, 3 mL of 0.079 M ascorbic acid was added. Then, 0.8 mL of the previously prepared gold seed solution was introduced into the growth solution. The resulting mixture was thoroughly shaken and allowed to stand for 1 hour.[1]

Synthesis of insulating matrix:

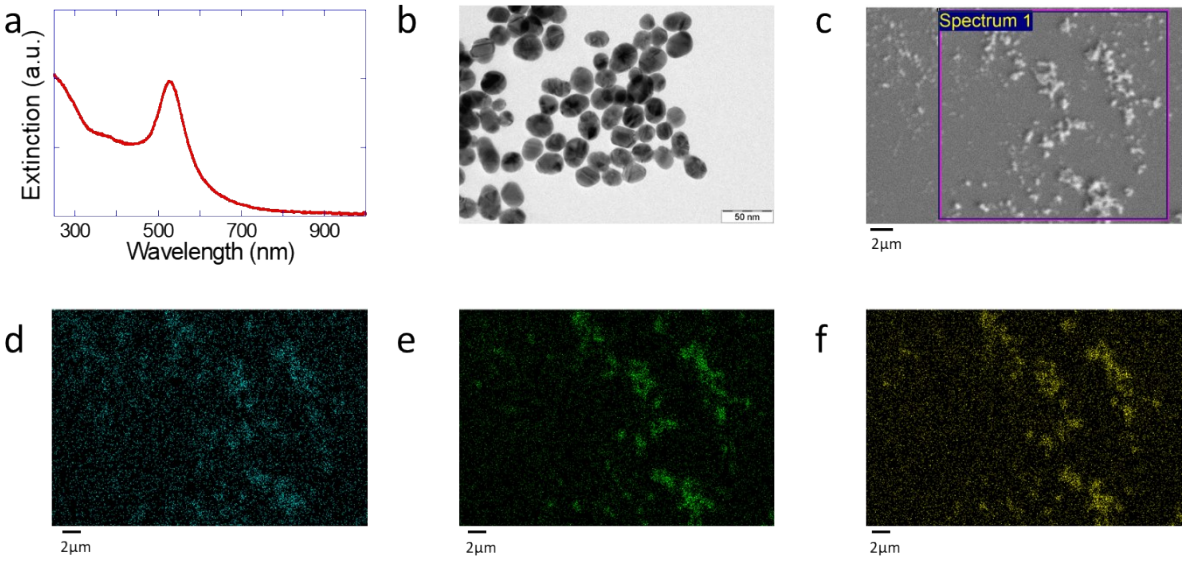

Figure S1: a. Optical spectrum of AuNS; b. TEM of AuNS; c. SEM of sample (region where the eds is done is highlighted); d., e., f. Au, Ag and Br signal from EDS

Au NS was cleaned and concentrated using centrifugation. Then it was diluted with mQ water so that

the final optical density is 0.1. 2mL of that was mixed with 1mL 2mM AgNO3 and 4mL H2O. Then it was irradiated with 100W white LED lamp for 24hrs. After that the precipitate is collected centrifuging it at 6000 RPM for 5 min.

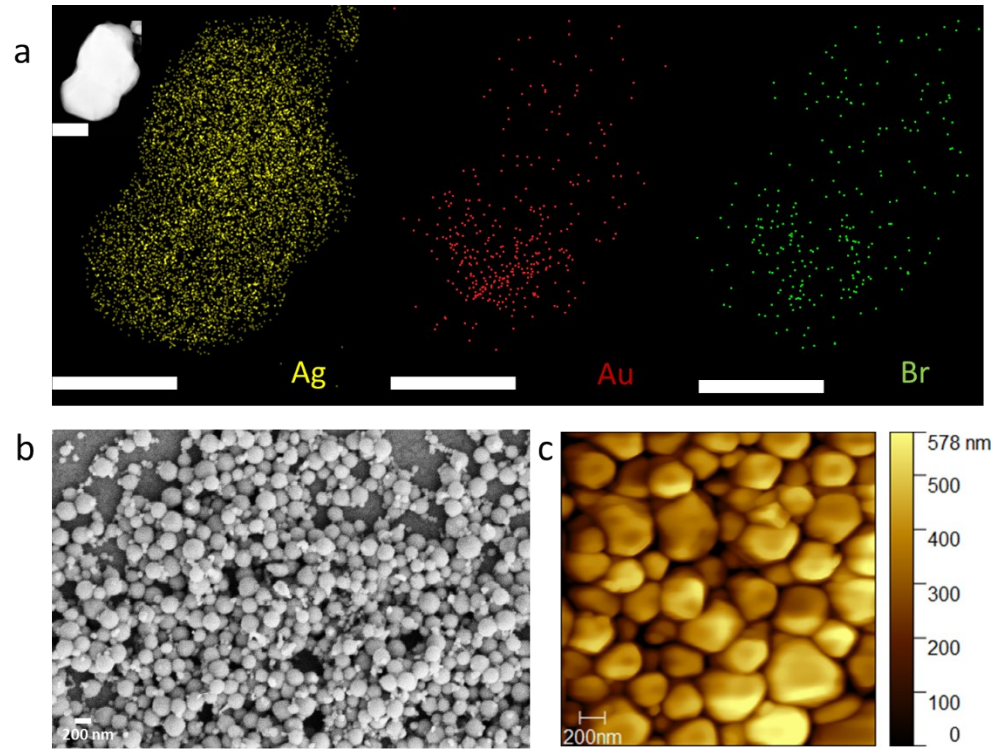

Figure S2: a. EDS signal of Ag, Au and Br respectively (HAADF in inset) from two closely spaced particles, Scalebar:100nm. Note: Particles tend to deform upon prolonged beam exposure[2,3]; b. SEM of nanoparticles, c. AFM of nanoparticles

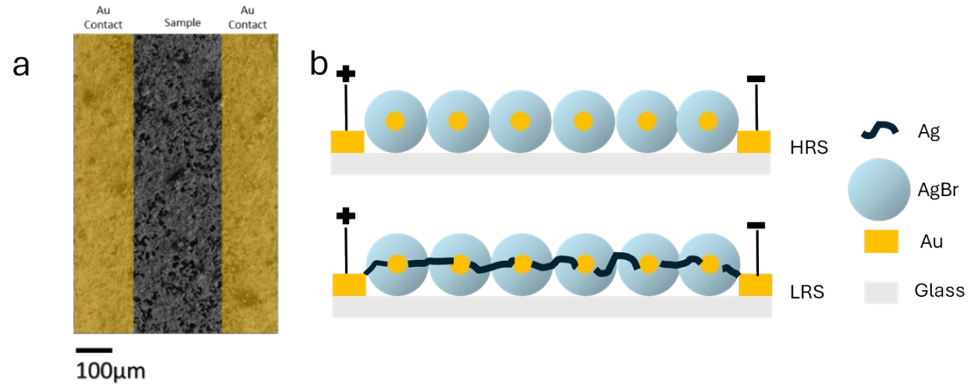

Figure S3: a. SEM of sample drop cast on patterned Au contacts (false colour), b. device schematic in the HRS and LRS

Device Fabrication:

A prepatterned Cr/Au contact of 15/150nm was sputtered on cleaned glass substrate using a shadow mask. The gap between two adjacent contacts were kept 200µm. On top of that particles were drop cast. A SEM image of the top view provided in false colour in Figure S3a and a schematic of cross sectional device architecture in its HRS and LRS is shown in Figure S3b. The granular material was chosen because this system shows emergent properties that are the subject of this work.

Section 2 (Electrical Measurements):

Electrical Measurement: All the electrical measurements were done using a Keithley-2450 SMU. The sample was connected to Keithley via probe station with two-point contact probes. Measurement setup schematic is shown in Figure S4 A power spectral density plot of the noise of Keithley-2450 is presented in Figure S5. Its log-log plot shows a slope of 0.98 when fitted to $PSD = \frac{10^k}{f^\alpha}$. This is significantly different from the slope we obtain in case of the noise of the device.

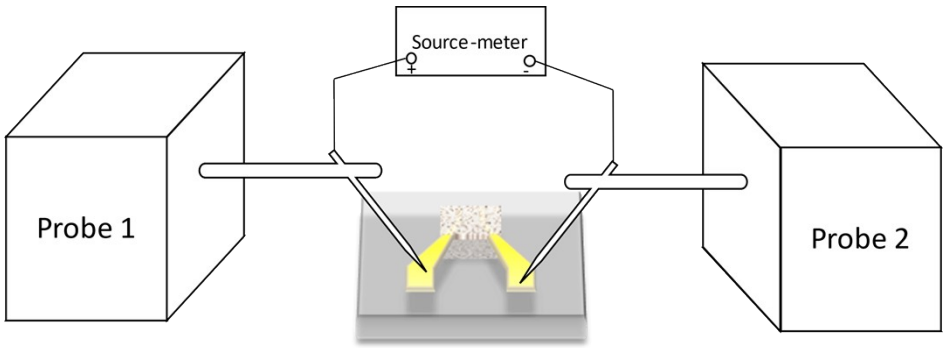

Figure S4: Measurement setup schematic

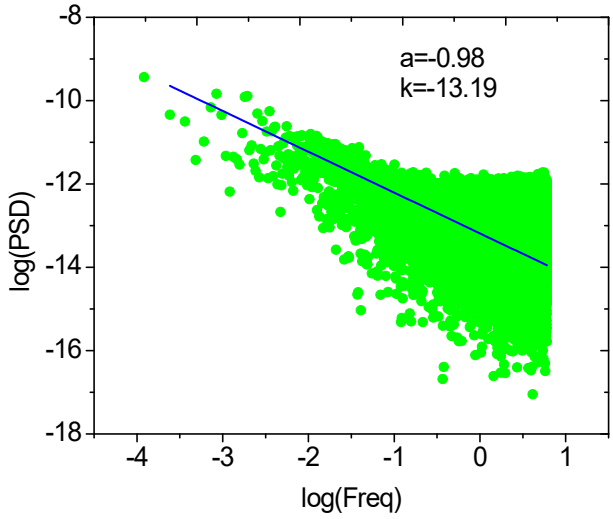

Figure S5: Power Spectral Density of the noise of Keithley 2450

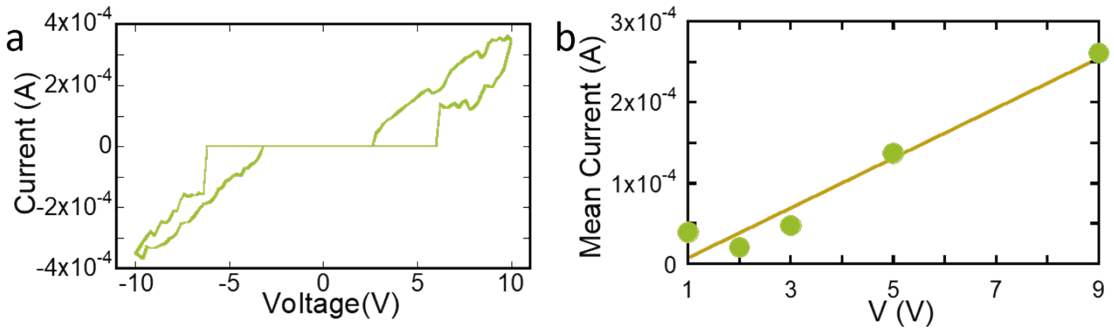

Figure S6: a. IV of the device within ±10V; b. Variation mean current with applied bias

Power law analysis threshold: The mean current is chosen to be the threshold. We have chosen the mean value as a threshold to enable comparison of ON/OFF statistics across different applied bias values. We note that as apparent from device characteristics shown in Figure S6a, current increases significantly with applied bias for the LRS. The use of the mean value as the threshold eliminates any artefacts arising from this effect. Variation of mean current with bias for a particular device is presented in Figure S6b.

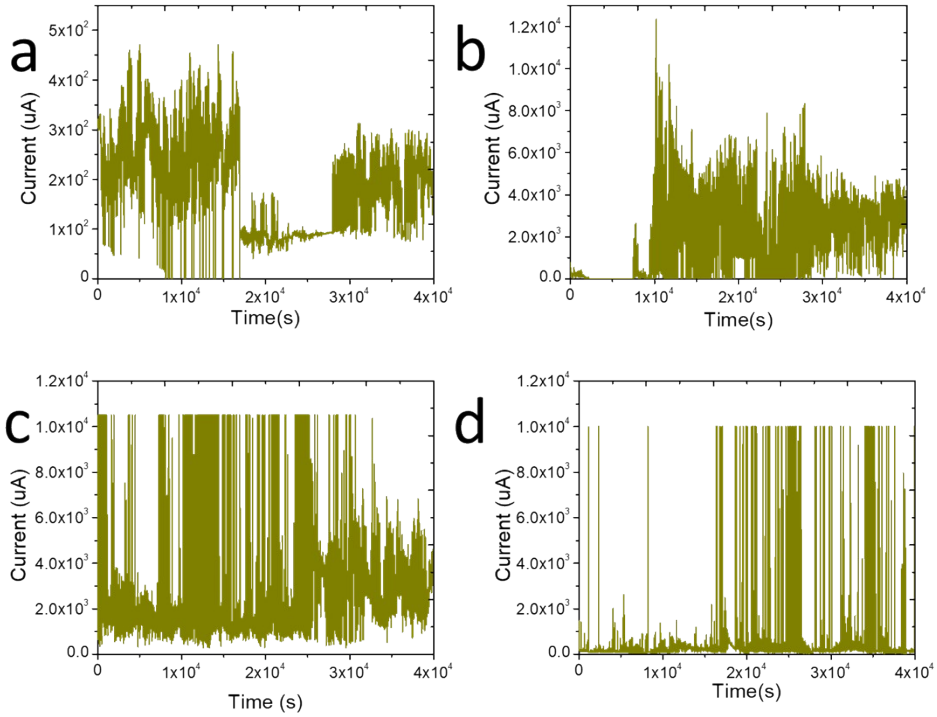

Figure S7: Current vs time at a. 2V; b. 3V; c. 5V; d. 9V

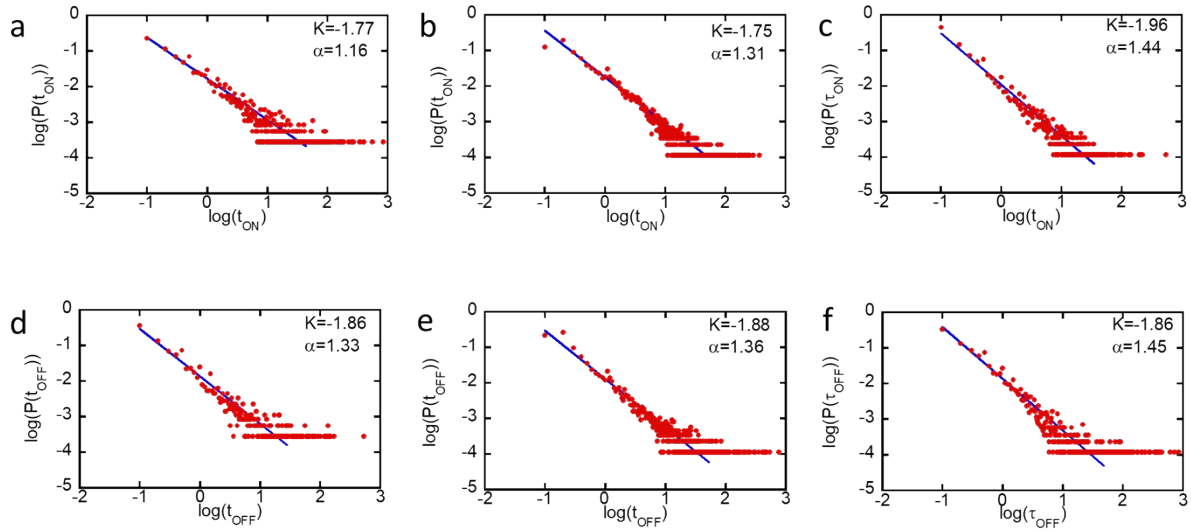

Figure S8: a., b., c. Power law analysis at ON state for 2V, 3V, 5V bias respectively; d., e., f. Power law analysis at OFF state for 2V, 3V and 5V bias respectively

Probing conversion of Ag during interchange between LRS and HRS: We show enhanced presence of halide in the HRS through UV-Vis and Raman. As can be seen from Figure 2a, the 320nm peak in UV-Vis reflectance of the sample in its high resistance state corresponds to silver halide present in the

device.[4] After transforming to its LRS, the peak is diminished confirming the reduction of silver halide to silver. This is also confirmed through the Raman spectrum where the silver halide features at 140 cm^{-1} and 200 cm^{-1} diminish in the LRS, consistent with conversion of silver halide.[5]

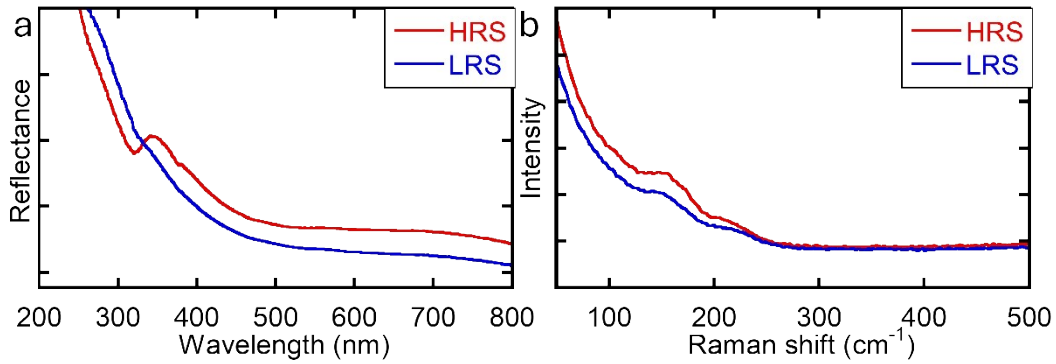

Figure S9: a. UV-Vis reflectance spectrum and b. Raman scattering from HRS and LRS. Silver halide absorption features in the HRS are evident at 320 nm in the reflectance. The appearance of this feature is also associated with increased Raman scattering at silver halide features from the HRS

Performance of memristor: A table and endurance plot for 60 cycles of three different devices are presented in Figure S10.

Switching Ratio (R_{OFF}/R_{ON})	~10^5
Average set voltage	2.8V, -3.95V
Average reset voltage	0.5V, -0.6V
Endurance	Behaves well till 60 cycles

Table S1: Performance of our sample as memristor

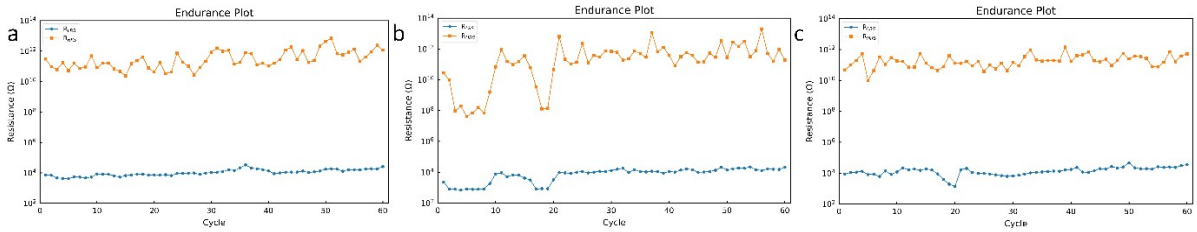

Figure S10: Endurance plot of 60 cycles of a, b. different devices of same batch of figure R3, c. device from a different batch

References:

1 N. R. Jana, L. Gearheart and C. J. Murphy, *Advanced Materials*, 2001, 13, 1389–1393.

2 R. Purbia and S. Paria, *Dalton Transactions*, 2017, 46, 890–898.

3 G. Loget, T. C. Lee, R. W. Taylor, S. Mahajan, O. Nicoletti, S. T. Jones, R. J. Coulston, V. Lapeyre, P. Garrigue, P. A. Midgley, O. A. Scherman, J. J. Baumberg and A. Kuhn, *Small*, 2012, 8, 2698–2703.

4 H. Zhang and M. Mostafavi, *J Phys Chem B*, 1997, 101, 8443–8448.

5 M. Assis, F. C. Groppo Filho, D. S. Pimentel, T. Robeldo, A. F. Gouveia, T. F. D. Castro, H. C. S. Fukushima, C. C. de Foggi, J. P. C. da Costa, R. C. Borra, J. Andrés and E. Longo, *ChemistrySelect*, 2020, 5, 4655–4673.